

01 Jan 1985

## Effects Of Iron Implantation On The Aqueous Corrosion Of Magnesium

S. Akavipat

Edward Boyd Hale

Missouri University of Science and Technology, ehale@mst.edu

C. E. Habermann

P. L. Hagans

Follow this and additional works at: [https://scholarsmine.mst.edu/phys\\_facwork](https://scholarsmine.mst.edu/phys_facwork)

 Part of the [Physics Commons](#)

---

### Recommended Citation

S. Akavipat et al., "Effects Of Iron Implantation On The Aqueous Corrosion Of Magnesium," *Materials Science and Engineering*, vol. 69, no. 2, pp. 311 - 316, Elsevier, Jan 1985.

The definitive version is available at [https://doi.org/10.1016/0025-5416\(85\)90328-3](https://doi.org/10.1016/0025-5416(85)90328-3)

This Article - Journal is brought to you for free and open access by Scholars' Mine. It has been accepted for inclusion in Physics Faculty Research & Creative Works by an authorized administrator of Scholars' Mine. This work is protected by U. S. Copyright Law. Unauthorized use including reproduction for redistribution requires the permission of the copyright holder. For more information, please contact [scholarsmine@mst.edu](mailto:scholarsmine@mst.edu).

## Effects of Iron Implantation on the Aqueous Corrosion of Magnesium\*

S. AKAVIPAT and E. B. HALE

Materials Research Center, and Department of Physics, University of Missouri-Rolla, Rolla, MO 65401 (U.S.A.)

C. E. HABERMANN and P. L. HAGANS

Central Research, Dow Chemical Company, Midland, MI 48640 (U.S.A.)

(Received September 17, 1984)

### ABSTRACT

*The influence of the implantation of iron ions on the corrosion of magnesium and an Al-Zn-rich magnesium alloy (AZ91C) has been studied. Anodic polarization measurements in a dilute chloride-containing alkaline solution were used to evaluate corrosion resistance. A range of ion energies (50–180 keV) and doses ( $10^{16}$ – $2 \times 10^{17}$  Fe<sup>+</sup> ions cm<sup>-2</sup>) have been evaluated. Both the iron-implanted pure magnesium and the alloy AZ91C gave improved polarization measurements. A systematic positive shift of the open-circuit potential with increasing iron dose was found. In AZ91C at a dose of  $10^{17}$  Fe<sup>+</sup> ions cm<sup>-2</sup>, there was a +0.6 V more noble shift in the open-circuit potential and a nearly equivalent shift of the pitting potential. In addition, there was a reduction of more than an order of magnitude in the current densities at all potentials. The ion energy did not have a large effect on the corrosion behavior. Annealing the samples did not further improve the corrosion resistance. The results from characterizing the corroded samples using Auger spectroscopy and scanning electron microscopy are also presented.*

### 1. INTRODUCTION

Corrosion of magnesium and its alloys in chloride-containing solutions is commonly observed and has been well studied [1–12]. Unless extremely pure samples are used, the

severity of the attack often is governed by small amounts of metallic impurities in the test specimens. This is especially true if the impurities are iron, nickel, cobalt or copper [1]. Since ion implantation can be used to implant such impurities, it is of interest to see how impurities introduced in this non-conventional way influence the corrosion of magnesium and its alloys.

In this paper, results on the influence of Fe<sup>+</sup> ion implantations into both high purity magnesium and one of its Al-Zn alloys (AZ91C) are presented. A variety of other metallic elements have also been implanted into magnesium and AZ91C. Most of these implantations did not favorably influence the corrosion resistance and have not been studied in detail. The favorable results of boron implantations have been previously presented [13], and they were the first corrosion results to be reported on ion-implanted magnesium. The iron results reported here are especially interesting as well as confusing. This is because iron in the bulk metal has a very *adverse* effect on the corrosion rate in chloride-containing solutions, while the implantation of iron ions has a *favorable* effect which is only slight in the pure metal but is strong in the AZ91C alloy.

### 2. EXPERIMENTAL PROCEDURES

The ultrapure samples were machined from slab stock of triply distilled magnesium into disks 19 mm in diameter and 3.2 mm thick. Similarly sized samples were also machined from AZ91C alloy ingots. This alloy contains 9 wt.% Al, 0.67 wt.% Zn, 0.08 wt.% Mn and only trace amounts of other impurities. The

\*Paper presented at the International Conference on Surface Modification of Metals by Ion Beams, Heidelberg, F.R.G., September 17–21, 1984.

aluminum and zinc are added to make a good casting alloy. The manganese is added to decrease the undesirable effect of iron impurities in magnesium alloys. The alloy is in its as-cast condition. This heat treatment produces easily identifiable regions of  $Mg_{17}Al_{12}$  compound in a predominantly magnesium matrix. The alloy is commercially used because of its good strength and formability. It also has favorable corrosion characteristics compared with magnesium metal.

The samples were highly polished using procedures described elsewhere [13] and were implanted in the Ion Implantation Laboratory, University of Missouri-Rolla. The samples were connected to a heat sink during implantation and current densities of  $1-3 \mu A cm^{-2}$  were used.

The corrosion measurements were made using apparatus and test procedures discussed in detail elsewhere [13, 14]. The electrolyte used was a borated boric acid solution containing 1000 ppm NaCl and had a pH of 9.3. The solution was deaerated with argon. The potential measurements were made relative to a Pd-H reference electrode. Typically, the sample was placed in the solution for several minutes to let the open-circuit potential stabilize. Then the potential was swept positive at a rate of  $1 mV s^{-1}$  until a sharp rise in the current density was observed. (Such a rise indicates that catastrophic breakdown has occurred in the protective layer.)

### 3. RESULTS

The first anodic polarization measurements were performed on a series of AZ91C alloy samples each of which had been exposed to a different dose of  $Fe^+$  ions. The results from these tests are shown in Fig. 1. At low doses, unfavorable results are seen at the higher current densities because the positive influence of the iron is not great enough to overcome the negative influence of the radiation damage.

The results on the high dose samples clearly show much improved corrosion resistance. This is not just because of the reduction of more than an order of magnitude in current density at all potentials but also because of the large positive (more noble) shift of the potential at which the corrosion current becomes very large.

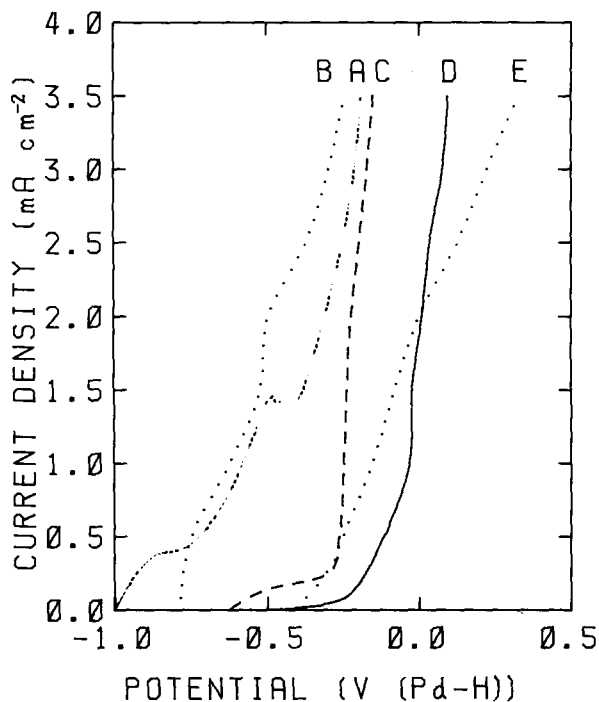


Fig. 1. Anodic polarization results from AZ91C alloy implanted with various doses of 100 keV  $Fe^+$  ions: curve A, unimplanted; curve B,  $1 \times 10^{16} Fe^+$  ions  $cm^{-2}$ ; curve C,  $5 \times 10^{16} Fe^+$  ions  $cm^{-2}$ ; curve D,  $10 \times 10^{16} Fe^+$  ions  $cm^{-2}$ ; curve E,  $20 \times 10^{16} Fe^+$  ions  $cm^{-2}$ . Under the same conditions, pure iron shows a breakdown potential of +0.82 V.

Examination of more samples has revealed that there is a systematic shift of the open-circuit potential  $E_{oc}$  with iron dose. ( $E_{oc}$  is the potential at which the anodic reaction rate is equal to that of the cathodic reaction rate.) The behavior of  $E_{oc}$  with dose is shown in Fig. 2. At the higher doses the data show that the shift can be as large as +0.6 V or more. It should be noted that this is an iron-specific effect rather than a radiation damage effect since there is little or no shift of  $E_{oc}$  with ions which are expected only to cause radiation damage, such as argon and magnesium. This systematic shift of the open-circuit potential to considerably more noble values was viewed as a positive effect.

To investigate further the effects of iron implantation, samples implanted at various energies were studied. Figure 3 shows that at similar doses there is a slight energy dependence of the pitting (*i.e.* breakdown) potential. This result is in sharp contrast with the corrosion improvements found when boron was implanted [13] where the lower energy

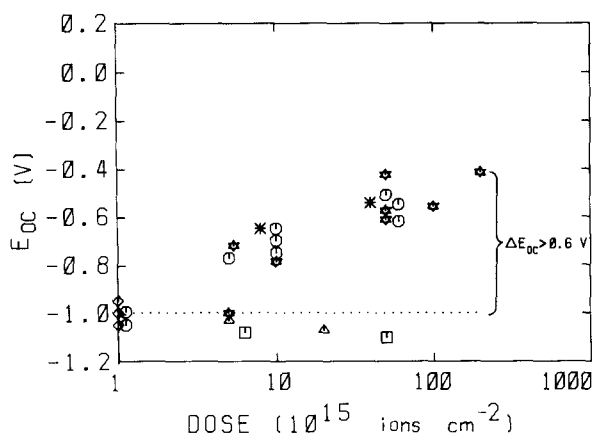


Fig. 2. Noble shift of the open-circuit potential  $E_{oc}$  in AZ91C alloy for various implant energies and ions;  $\diamond$ , unimplanted;  $*$ , 50 keV  $Fe^+$  ions;  $\odot$ , 100 keV  $Fe^+$  ions;  $\odot$ , 180 keV  $Fe^+$  ions;  $\triangle$ , 100 keV  $Mg^+$  ions;  $\square$ , 100 keV  $Ar^+$  ions. Iron implants cause large shifts while magnesium and argon implants do not. On the potential scale used in the figure, pure iron has an open-circuit potential  $E_{oc}$  of +0.32 V.

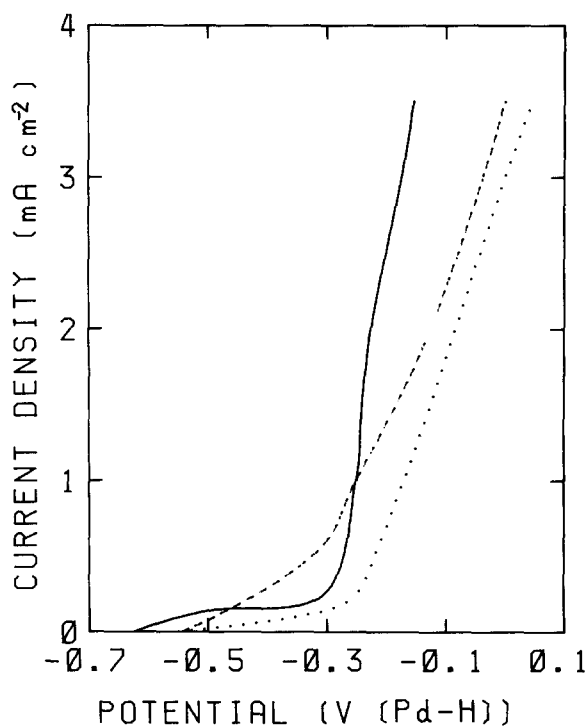


Fig. 3. Polarization results for fixed iron dose ( $5 \times 10^{16} Fe^+$  ions  $cm^{-2}$ ) implants into AZ91C alloy at various ion energies: -----, 50 keV; —, 100 keV; ..... , 180 keV.

implantations were found to be more effective. Such an energy dependence suggests that the boron is mostly effective in the near-surface, presumably in the passivating layer.

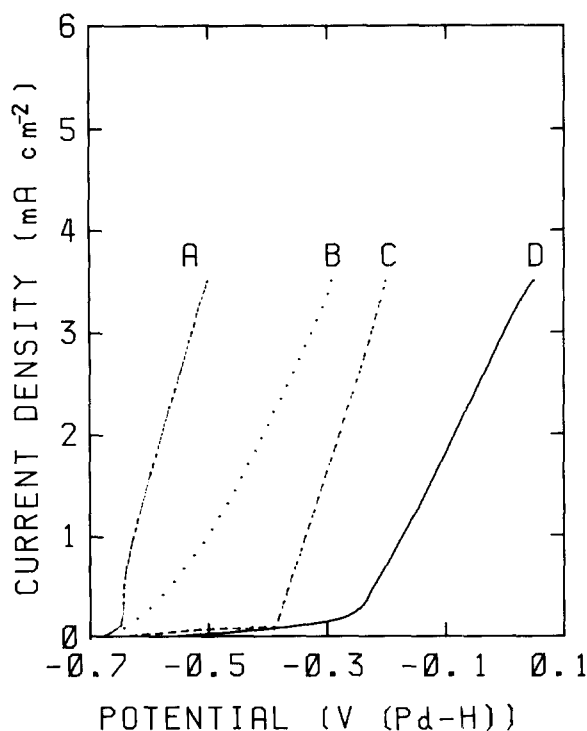


Fig. 4. Influence of annealing on polarization results in an AZ91C sample implanted with  $5 \times 10^{16} Fe^+$  ions  $cm^{-2}$  at 180 keV: curve D, as implanted; curve C, annealed for 3 h at 175 °C; curve B, annealed for 18 h at 250 °C; curve A, annealed for 2 h at 500 °C.

However, the depth dependence in the iron case suggests that the iron may be mobile and that kinetics are playing a greater role in the iron case.

To test the influence of thermal kinetics, several samples were annealed at various temperatures after identical implantations and prior to corrosion testing. The annealing can both reduce any residual radiation damage as well as alter the state of the iron. The results are shown in Fig. 4. The figure shows that the annealing basically reduces the corrosion-inhibiting effect of the iron. There is clearly a systematic worsening of the breakdown potential, although the open-circuit voltage still remains improved over the unimplanted case.

Auger measurements have been made to examine the implanted samples both before and after corrosion. Figure 5 shows the results of these measurements. The implanted iron has a more or less gaussian depth distribution, with the range of the iron at 100 keV being slightly greater than the thickness of the oxide layer (see Fig. 5(a)). The Auger mea-

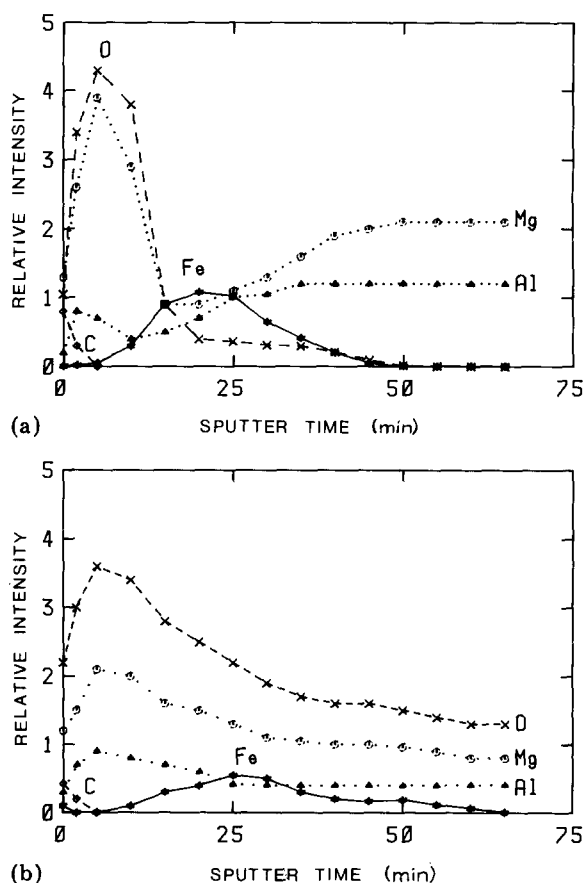


Fig. 5. Depth profiles obtained from Auger measurements on an AZ91C sample implanted with  $5 \times 10^{16}$   $\text{Fe}^+$  ions  $\text{cm}^{-2}$  at 100 keV (the sputter rate removes  $35 \text{ \AA min}^{-1}$  of a  $\text{Ta}_2\text{O}_5$  film): (a) from an uncorroded region of the sample; (b) from a corroded region of the sample.

measurements for implantation at 180 keV show that the peak in the iron distribution is much deeper and that the iron extends out through the oxide to the surface. Such a distribution supports the above conjecture that the iron has some mobility after it is implanted.

The Auger results on the sample after exposure to the full potential sweep of the anodic polarization test are given in Fig. 5(b). A thick hydroxide layer has now formed on the surface. Visually, it is clear that severe corrosion has occurred, but the figure shows that most, if not all, the iron has been retained in the surface layer. This is in sharp contrast with the boron-implanted case in which severe corrosive attack removed the boron [13].

To characterize more fully the corrosive attack, samples exposed to various stages of the anodic polarization sweep have been

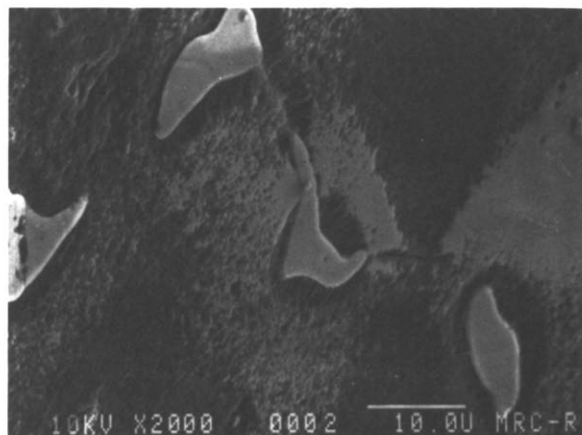


Fig. 6. Micrograph of corroded unimplanted AZ91C alloy swept to  $-0.45 \text{ V}$ . The white islands are an  $\text{Mg}_{17}\text{Al}_{12}$  compound formed in the aluminum-saturated magnesium background matrix.

studied using a scanning electron microscope. This study revealed that the breakdown which leads to the very high current densities (greater than  $2 \text{ mA cm}^{-2}$ ) in both the unimplanted and the implanted samples appears to be caused by the same phenomenon, namely the formation of large-diameter (about  $50\text{--}100 \mu\text{m}$ ) pits which are also quite deep. However, corrosion conditions at lower current densities were quite different in the unimplanted and implanted samples.

Figure 6 shows the corrosive attack on an unimplanted sample which was anodically swept to the middle of the  $1.5 \text{ mA cm}^{-2}$  passivation plateau (see Fig. 1). There has been serious localized attack to form a deep moat around the " $\text{Mg}_{17}\text{Al}_{12}$  islands" found in the AZ91C alloy. (These islands were formed when the alloy is cast.) However, Fig. 7 shows that no such attack occurs in the implanted samples which were anodically swept to the same voltage ( $-0.45 \text{ V}$ ). Instead, the islands themselves are attacked and black corrosion spots develop on the islands. No severe attack occurred in the solid solution regions between the islands.

The results for AZ91C led us to explore the corrosion behavior of iron-implanted pure (triply distilled) magnesium. Figure 8 shows the corrosion behavior of triply distilled samples implanted with different doses of iron. The implantation has somewhat reduced the corrosion current density and has increased the open-circuit potential by several

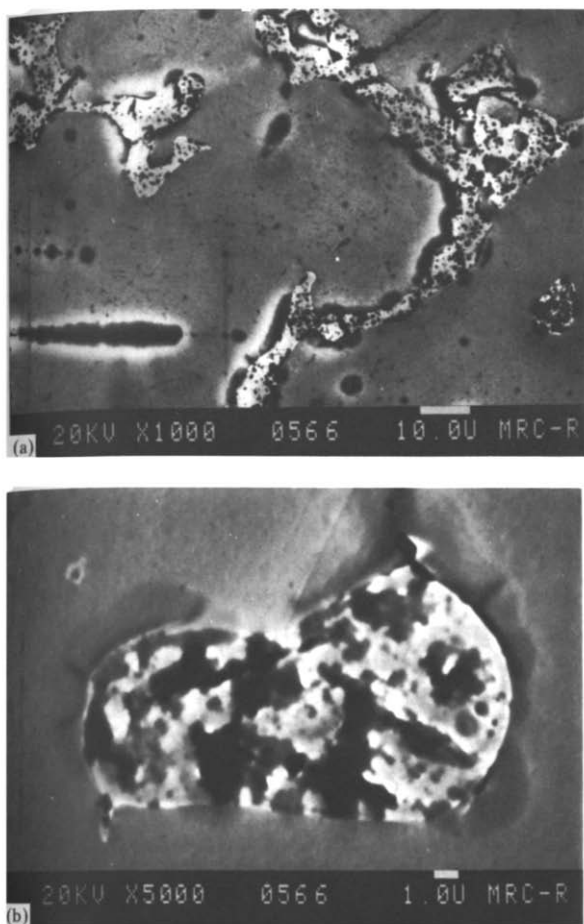


Fig. 7. Micrographs of corroded AZ91C alloy implanted with  $5 \times 10^{16}$   $\text{Fe}^+$  ions  $\text{cm}^{-2}$  at 100 keV swept to  $-0.45$  V: (a) overall view; (b) detailed picture of an island. The implantation has significantly reduced the localized attack at the island-matrix interface. Instead, the attack has been transferred to the  $\text{Mg}_{17}\text{Al}_{12}$  islands and is less severe. (Compare with Fig. 6.)

tenths of a volt. However, the improvement in the triply distilled case is not as clear cut or as dramatic as it was for AZ91C.

#### 4. DISCUSSION

The enhanced corrosion of magnesium and its alloys caused by trace amounts of iron is well known. It is such a classic example of the effect that impurities can have on accelerating corrosion that it is used in textbooks, such as ref. 15. The influence of iron on the corrosion rate was seen in pure magnesium [1] beginning at a concentration of 0.017 wt.% and in an Mg-Al alloy the influence of iron began

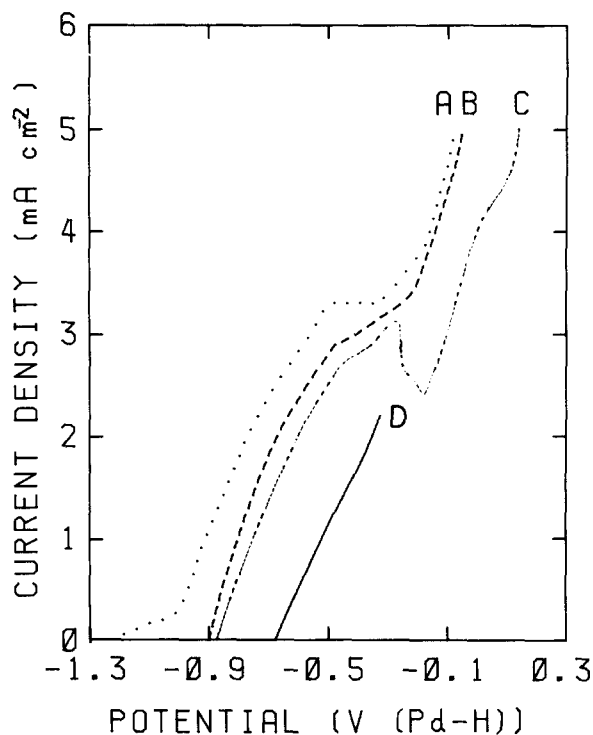


Fig. 8. Anodic polarization results from triply distilled magnesium implanted with various  $\text{Fe}^+$  ion doses at 100 keV: curve A, unimplanted; curve B,  $1 \times 10^{16}$   $\text{Fe}^+$  ions  $\text{cm}^{-2}$ ; curve C,  $5 \times 10^{16}$   $\text{Fe}^+$  ions  $\text{cm}^{-2}$ ; curve D,  $10 \times 10^{16}$   $\text{Fe}^+$  ions  $\text{cm}^{-2}$ . (There were instrumental problems with the curve D run, but the results in the early part of the run are believed to be accurate).

below the detectable limit (less than 0.0002 wt.%). Manganese stabilized this so-called "tolerance limit" to 0.002 wt.% in AZ91C alloys [1], but this limit is an order of magnitude below the pure magnesium limit quoted above.

There are no specific theories as to why iron causes such enhanced corrosion in magnesium. However, iron and certain other transition metals, such as nickel and cobalt, which have a low hydrogen overvoltage all accelerate corrosion in magnesium, while other impurities which do not evolve hydrogen easily have considerably less influence on the corrosive attack. The net effect is that iron impurities enhance a cathodic reaction which evolves hydrogen and promote an anodic reaction which enhances magnesium corrosion.

The sensitivity of the corrosion to implants of iron ions is very different and, in fact, is "doubly reversed" from conventionally intro-

duced iron. This is because not only does the implanted iron reduce the corrosion rate in both the triply distilled magnesium and AZ91C cases but also it is much more effective in AZ91C. Clearly, the implanted iron has introduced major changes in the conventional corrosion mechanisms caused by impurities.

In the early stages of corrosion (*i.e.* at the lower current densities), Figs. 6 and 7 clearly demonstrate that there are major differences between the corrosive attack in the unimplanted samples and that in the implanted samples. In the unimplanted case (Fig. 6), it appears that the  $Mg_{17}Al_{12}$  islands acted as cathodic sites and locally enhanced the anodic reaction in the magnesium matrix. Thus a deep moat has been locally corroded from the matrix about each island.

In the implanted case (Fig. 7) the effect of the implantation has been mainly to confine the corrosion to small localized regions which are in the islands. The less severe attack, coupled with the fact that the  $Mg_{17}Al_{12}$  compound occupies only a small fraction (10%–15%) of the volume of the alloy, results in much lower corrosion currents. In addition, shifting the corrosion mainly to the islands is a favorable result because the islands are isolated and only extend several microns below the surface. Thus there is no direct path which could lead to undesirable deep corrosion.

In the catastrophic stage of corrosion, there have been major breakdowns in the thick hydroxide protective layer formed in the early stages of corrosion. In the breakdown regions, large corrosive pits are observed in both the unimplanted and the implanted samples. Thus in this case the influence of the implanted iron has not been to change the corrosive mechanism. However, the iron apparently influences the nature of the protective film. The resulting effect is to improve the corrosion resistance by changing the initial breakdown conditions in the film. Thus a major shift of the breakdown potential to substantially more noble values is observed (see Fig. 1).

## 5. CONCLUSIONS

Iron implantation has been used to modify the corrosion behavior of magnesium and an

Mg–Al alloy in a chloride-containing solution. Major improvements in the corrosion resistance were found in the implanted alloy as described below.

Anodic polarization measurements showed that iron implantation greatly reduces the corrosion current densities at all applied voltages less than the breakdown potential of the protective film. In addition, this breakdown potential and the open-circuit potential were shifted several tenths of a volt more noble as a result of the implantation. Prior to catastrophic breakdown the electron microscope results show clearly that the effect of the implantation was to modify the dominant mechanism from a rather severe local attack at the interface of the two metallic phases in the alloy to a much more localized and less severe attack on the smaller  $Mg_{17}Al_{12}$  phase.

## REFERENCES

- 1 J. D. Hanawalt, C. E. Nelson and J. A. Peloubet, *Trans. AIME*, 147 (1942) 273.
- 2 W. S. Loose, in H. H. Uhlig (ed.), *Corrosion Handbook*, Wiley, New York, 1948, pp. 218–252.
- 3 G. R. Hoey and M. Cohen, *J. Electrochem. Soc.*, 105 (1958) 245.
- 4 R. Glicksman, *J. Electrochem. Soc.*, 106 (1959) 457.
- 5 J. L. Robinson and P. F. King, *J. Electrochem. Soc.*, 108 (1961) 36.
- 6 L. Whitby, F. L. LaQue and H. R. Copson (eds.), *Corrosion Resistance of Metals and Alloys*, Reinhold, New York, 1963, Chapter 7.
- 7 M. E. Straumanis and B. K. Bhatia, *J. Electrochem. Soc.*, 110 (1963) 357.
- 8 P. F. King, *J. Electrochem. Soc.*, 110 (1963) 1113.
- 9 P. F. King, *J. Electrochem. Soc.*, 113 (1966) 536.
- 10 J. W. Johnson, C. K. Chi and W. J. James, *Corrosion*, 23 (1967) 204.
- 11 G. G. Perault, *J. Electroanal. Chem.*, 27 (1970) 47.
- 12 R. Tunold, H. Holtan, M. H. Berge, A. Lasson and R. Steen-Hansen, *Corros. Sci.*, 17 (1977) 353.
- 13 S. Akavipat, C. E. Habermann, P. L. Hagans and E. B. Hale, in E. McCafferty, C. R. Clayton and J. Oudar (eds.), *Proc. Int. Symp. on Fundamental Aspects of Corrosion Protection by Surface Modification*, Washington, DC, October 9–14, 1983, in *Spec. Publ. 84-3*, 1984, pp. 52–61 (Corrosion Division, Electrochemical Society, Pennington, NJ).
- 14 P. L. Hagans, *Proc. International Magnesium Association 1984 Annu. Meet., London, 1984*, to be published.
- 15 *NACE Basic Corrosion Course*, National Association of Corrosion Engineers, Houston, TX, 1970, Chapter 11, p. 16.